

Modulated optical vortices

Jennifer E. Curtis ¹ and David G. Grier

Dept. of Physics, James Franck Institute and Institute for Biophysical Dynamics

The University of Chicago, Chicago, IL 60637

Single-beam optical gradient force traps created by focusing helical modes of light are known as optical vortices. Modulating the helical pitch of such a modes' wavefront yields a new class of optical traps whose dynamically reconfigurable intensity distributions provide new opportunities for controlling motion in mesoscopic systems. This Letter describes an implementation of modulated optical vortices based on the dynamic holographic optical tweezer technique. © 2004 Optical Society of America

OCIS codes: 140.7010, 090.1760, 350.5030, 350.3850

A single-beam optical gradient force trap, known as an optical tweezer, is created by focusing a beam of light with a strongly converging high-numerical-aperture lens.¹ Optical tweezers can trap and move materials noninvasively at lengthscales ranging from tens of nanometers to tens of micrometers, and so have provided unprecedented access to physical, chemical and biological processes in the mesoscopic domain.² Variants of optical tweezers based on specially crafted modes of light have demonstrated additional useful and interesting properties: optical vortices created from helical modes of light exert torques on trapped objects,³⁻¹¹ traps based on Bessel

¹Present Address: Physikalische-Chemie Institut, Universität Heidelberg

beams facilitate controlled transport over long distances,¹² and optical rotators provide fine orientation control.¹³ These specialized traps have potentially widespread applications in biotechnology¹⁴ and micromechanics,¹⁵ particularly when created as integrated optical systems using holographic techniques.¹⁶ This Letter introduces a generalized class of optical vortices with novel properties, and describes their implementation as dynamic holographic optical traps.¹⁶

A vortex-forming helical mode is distinguished from a plane wave by an overall phase factor, $\exp(i\ell\theta)$, where θ is the polar angle in the plane normal to the optical axis and ℓ is an integral winding number that characterizes the beam's helical topology. The phase modulation $\varphi_\ell(\theta) = \ell\theta$ transforms the wavefront into an ℓ -fold helix winding around the optical axis. Semiclassical theory suggests that each photon in a helical beam carries an orbital angular momentum $\ell\hbar$, distinct from the photon's intrinsic spin angular momentum, and yet quantized in units of Planck's constant.^{10,17} This has been confirmed through measurements of particles' motions in optical vortices.^{4,6,8,18,19} The topological charge ℓ also determines the annular intensity distribution characteristic of an optical vortex.^{17,19,20} Because all phases appear along a helical beam's axis, destructive interference suppresses the axial intensity. Similarly, each ray at a radius r from the axis has an out-of-phase counterpart with which it destructively interferes when the beam is converged with a lens. Consequently, an optical vortex's core is dark, the beam's intensity being redistributed to an annulus at radius R_ℓ from the focal point.

Recently, we demonstrated that the radius of an optical vortex scales linearly

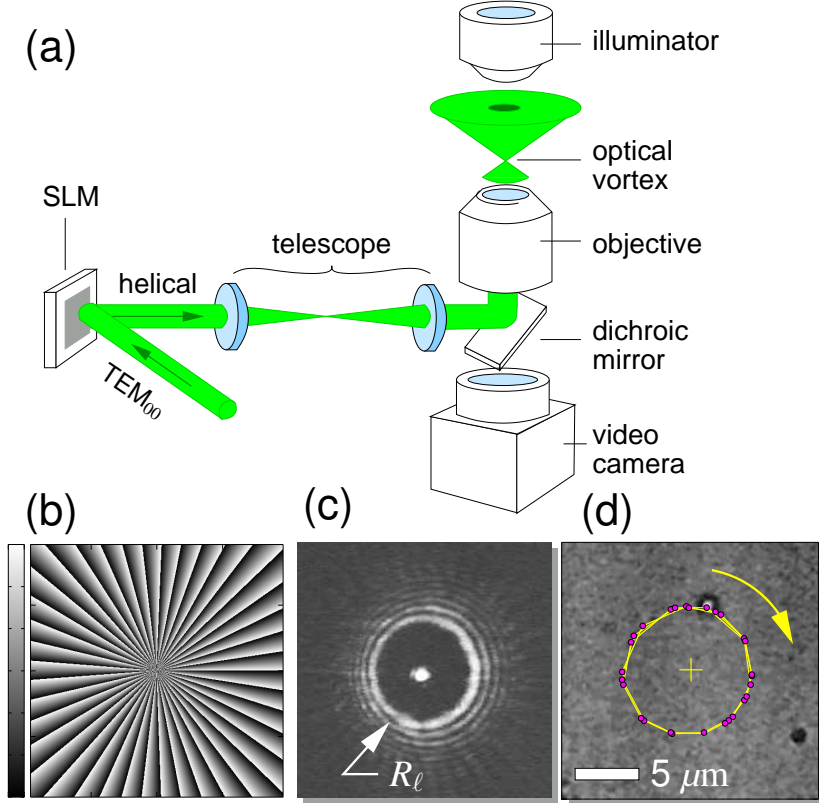


Fig. 1. Creating optical vortices with dynamic holographic optical tweezers.

(a) Schematic diagram of the experimental apparatus. A reflective spatial light modulator imprints the phase modulation $\varphi(\vec{r})$ onto the wavefront of a TEM_{00} laser beam. The transformed beam is relayed by a telescope to the back aperture of a microscope objective lens that focuses it into an optical trap. A conventional illuminator and video camera create images of objects in the trap. (b) The phase modulations encoding an $\ell = 40$ optical vortex. (c) The resulting optical vortex's intensity in the focal plane. (d) Trajectory of a single 800 nm diameter silica sphere traveling around the optical vortex's circumference, measured at 1/6 second intervals over 5 seconds.

with topological charge:^{19,21}

$$R_\ell \approx a \frac{\lambda}{\text{NA}} \left(1 + \frac{\ell}{\ell_0} \right), \quad (1)$$

where λ is the wavelength of light, NA is the objective lens' numerical aperture, and the constants a and ℓ_0 depend on the beam's radial amplitude profile. This observation suggests the generalization

$$R(\theta) = a \frac{\lambda}{\text{NA}} \left[1 + \frac{1}{\ell_0} \frac{d\varphi(\theta)}{d\theta} \right] \quad (2)$$

in which the local radius of maximum intensity at angle θ in the plane of the optical vortex depends on the “local winding number”. For example, choosing

$$\varphi(\theta) = \ell [\theta + \alpha \sin(m\theta + \beta)] \quad (3)$$

might be expected to produce an m -fold symmetric Lissajous pattern whose depth of modulation is controlled by α and whose orientation depends on β . Direct visualization using the dynamic holographic optical tweezer technique¹⁶ confirms this prediction, and thus verifies Eq. (2).

Our optical trapping system, shown in Fig. 1(a), has been described in detail elsewhere.^{16,19} We use a reflective liquid crystal spatial light modulator (SLM)²² to imprint a desired phase profile $\varphi(\mathbf{r})$ onto the wavefront of a collimated TEM₀₀ beam of light ($\lambda = 532$ nm). The modified beam is relayed to the input pupil of a high-NA objective lens mounted in an inverted light microscope. A mirror placed in the lens' focal plane reflects the resulting intensity distribution back down the optical axis to form an image on an attached video camera. Figure 1(b) shows a typical phase mask encoding an optical vortex with $\ell = 40$, and Fig. 1(c) shows the resulting intensity

distribution. The SLM has a diffraction efficiency of roughly 50%, and the central spot in Fig. 1(c) is a conventional optical tweezer centered on the optical axis formed from the undiffracted portion of the input beam. Because the SLM can only impose phase shifts in the range 0 to 2π radians, the projected phase function wraps around at $\varphi = 2\pi$ to create a scalloped appearance.

When an optical vortex is projected into a sample of colloidal microspheres dispersed in water, optical gradient forces draw spheres onto the ring of light, and the beam's orbital angular momentum drives them around the circumference, as shown in Fig. 1(d). The resulting motion entrains a flow of both fluid and particles in a way that has yet to be studied systematically, but whose qualitative features suggest opportunities for pumping and mixing extremely small sample volumes.

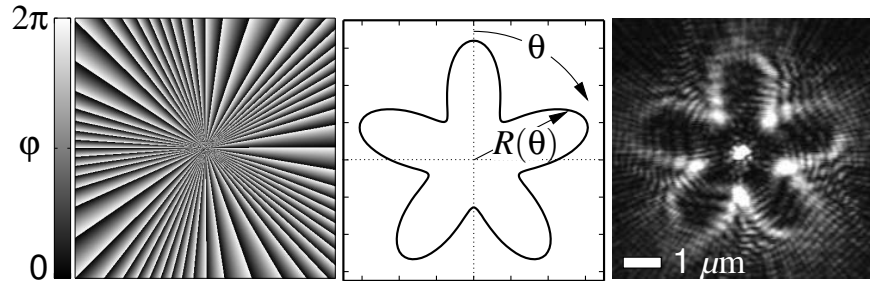


Fig. 2. Modulated optical vortex with $m = 5$, $\alpha = 0.1$. (a) Phase modulation. (b) Predicted radial profile $R(\theta)$. (c) Experimental intensity distribution.

Figure 2 shows how periodically modulating an optical vortex's phase affects its geometry. The phase mask in Fig. 2(a) includes an $m = 5$ fold modulation of amplitude $\alpha = 0.1$ superimposed on an $\ell = 60$ helical pitch. The radial profile predicted with Eq. (2) appears in Fig. 2(b) and agrees well with the observed intensity dis-

tribution in Fig. 2(c). Comparably good agreement is obtained with our apparatus for modulated helical phases up to $m = 12$ and $\alpha = 1$ and $\ell = 60$. Figure 3 shows typical intensity patterns obtained by varying m with fixed depth of modulation α , and by varying α with fixed m . Increasing the modulation beyond $\alpha_c = (\ell_0/\ell + 1)/m$ causes the locus of maximum intensity to pass through the origin and to create lobes of negative parity, as shown in the last two images in Fig. 3.

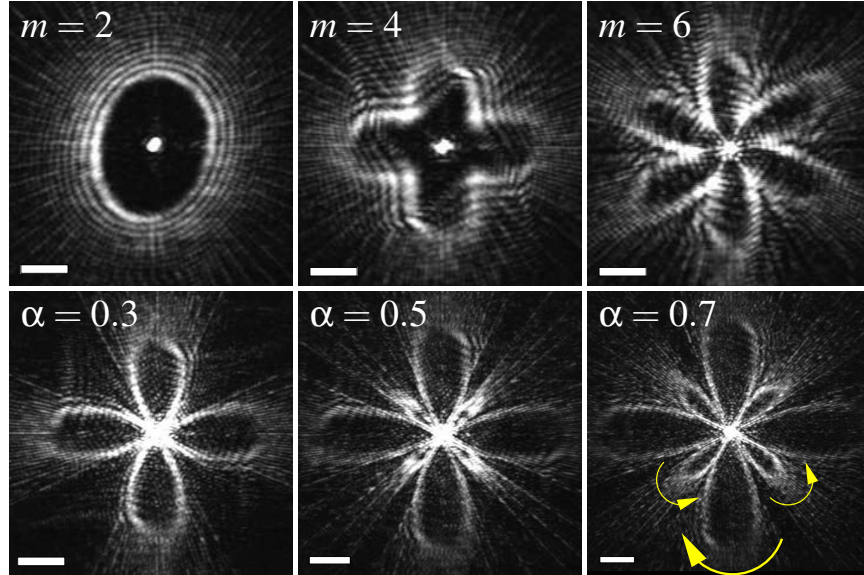


Fig. 3. Modulated optical vortices at $\alpha = 0.1$ with $m = 2, 4$, and 6 , (top) and at $m = 4$ with $\alpha = 0.3, 0.5$, and 0.7 (bottom). Additional lobes appear in the lower patterns for $\alpha > \alpha_c \approx 0.25$ with the direction of tangential forces indicated by arrows. All patterns were created with $\ell = 60$. Scale bars indicate $1 \mu\text{m}$.

Just as uniform optical vortices exert torques on trapped particles, modulated optical vortices exert tangential forces. These forces can drive particles through quite

complicated trajectories, as demonstrated in Fig. 4. Here, two 800 nm diameter polystyrene spheres dispersed in water are shown circulating around a three-fold modulated optical vortex, each completing one circuit in about two seconds. Whereas spheres travel more or less uniformly around a conventional optical vortex,¹⁹ such as the example in Fig. 1, they tend to circulate most rapidly where $R(\theta)$ is smallest in modulated patterns. This arises both because the light is most intense at smaller radii, and also because artifacts due to the SLM's finite spatial resolution¹⁹ tend to have a more pronounced effect on the traps' structures at larger radii. Diminishing intensities at larger radii also tend to weaken the traps at deeper modulations such as those shown in Fig. 3. Deeply modulated patterns tend to project particles transverse to the beam, rather than circulating them. Such optically mediated distribution could be useful for manipulating samples in microfluidic devices. Unlike distribution methods based on translating discrete optical tweezers,²³ the present approach can be implemented with a single static diffractive optical element.

In addition to translating particles, the forces exerted by modulated optical vortices can be used to distinguish particles on the basis of their size, shape, and optical properties. Consequently, modulated optical vortices may also provide a basis for sorting and fractionating mesoscopically sized materials,²⁴ applications that will be described elsewhere.

A modulated optical vortex can be rotated to any angle by varying β in Eq. (3). An asymmetric object comparable in extent to the trapping pattern can be immobilized on the pattern's asperities, and its orientation controlled by varying the phase angle. The negative-parity lobes of deeply modulated optical vortices exert retrograde

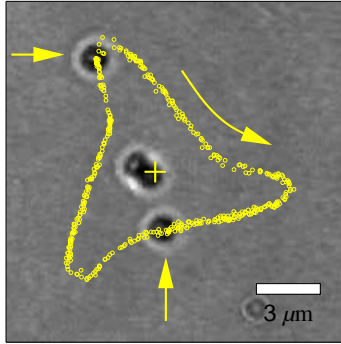


Fig. 4. Two particles' transit around a modulated optical vortex. Data points show the positions of two 800 nm diameter polystyrene spheres measured at 1/10 sec intervals over 10 sec. The two spheres, indicated by arrows, move along a trap with $\ell = 60$, $m = 3$, and $\alpha = 0.1$ at 300 mW, in the direction indicated by the curved arrow. Two additional spheres are trapped motionlessly in the undiffracted central spot.

tangential forces useful for canceling the overall torque on large illuminated objects. Comparable controlled rotation has been implemented by interfering an optical vortex with a conventional optical tweezer,¹³ and by creating optical traps with elliptically polarized light.²⁵ The present approach offers several advantages: the trapped object can be oriented by a single beam of light without mechanical adjustments; the intensity distribution can be tailored to the targeted sample's shape through Eq. (2); and the same apparatus can create multiple independent rotators simultaneously.¹⁶ These enhanced capabilities suggest applications for modulated optical vortices in actuating microelectromechanical systems (MEMS) such as pumps and valves in microfluidic and lab-on-a-chip devices.

This work was supported by the Materials Research Science and Engineering Center program of the National Science Foundation through Grant DMR-9880595.

References

1. A. Ashkin, J. M. Dziedzic, J. E. Bjorkholm, and S. Chu, “Observation of a single-beam gradient force optical trap for dielectric particles,” *Opt. Lett.* **11**, 288–290 (1986).
2. A. Ashkin, “History of optical trapping and manipulation of small-neutral particle, atoms, and molecules,” *IEEE J. Sel. Top. Quantum Elec.* **6**, 841–856 (2000).
3. H. He, N. R. Heckenberg, and H. Rubinsztein-Dunlop, “Optical particle trapping with higher-order doughnut beams produced using high efficiency computer generated holograms,” *J. Mod. Opt.* **42**, 217–223 (1995).
4. H. He, M. E. J. Friese, N. R. Heckenberg, and H. Rubinsztein-Dunlop, “Direct observation of transfer of angular momentum to absorptive particles from a laser beam with a phase singularity,” *Phys. Rev. Lett.* **75**, 826–829 (1995).
5. N. B. Simpson, L. Allen, and M. J. Padgett, “Optical tweezers and optical spanners with Laguerre-Gaussian modes,” *J. Mod. Opt.* **43**, 2485–2491 (1996).
6. M. E. J. Friese, J. Enger, H. Rubinsztein-Dunlop, and N. R. Heckenberg, “Optical angular-momentum transfer to trapped absorbing particles,” *Phys. Rev. A* **54**, 1593–1596 (1996).
7. K. T. Gahagan and G. A. Swartzlander Jr., “Optical vortex trapping of particles,” *Opt. Lett.* **21**, 827–829 (1996).
8. H. Rubinsztein-Dunlop, T. A. Nieminen, M. E. J. Friese, and N. R. Heckenberg,

“Optical trapping of absorbing particles,” *Adv. Quantum Chem.* **30**, 469–492 (1998).

9. K. T. Gahagan and G. A. Swartzlander, “Simultaneous trapping of low-index and high-index microparticles observed with an optical-vortex trap,” *J. Opt. Soc. Am. B* **16**, 533–537 (1999).

10. L. Allen, M. J. Padgett, and M. Babiker, “The orbital angular momentum of light,” *Prog. Opt.* **39**, 291–372 (1999).

11. A. T. O’Neil and M. J. Padgett, “Three-dimensional optical confinement of micron-sized metal particles and the decoupling of the spin and orbital angular momentum within an optical spanner,” *Opt. Comm.* **185**, 139–143 (2000).

12. J. Arlt, V. Garces-Chavez, W. Sibbett, and K. Dholakia, “Optical micromanipulation using a Bessel light beam,” *Opt. Comm.* **197**, 239–245 (2001).

13. L. Paterson, M. P. MacDonald, J. Arlt, W. Sibbett, P. E. Bryant, and K. Dholakia, “Controlled rotation of optically trapped microscopic particles,” *Science* **292**, 912–914 (2001).

14. W. He, Y. G. Liu, M. Smith, and M. W. Berns, “Laser microdissection for generation of a human chromosome region-specific library,” *Microscopy Microanalysis* **3**, 47–52 (1997).

15. M. E. J. Friese, H. Rubinsztein-Dunlop, J. Gold, P. Hagberg, and D. Hanstorp, “Optically driven micromachine elements,” *Appl. Phys. Lett.* **78**, 547–549 (2001).

16. J. E. Curtis, B. A. Koss, and D. G. Grier, “Dynamic holographic optical tweezers,” *Opt. Comm.* **207**, 169–175 (2002).

17. L. Allen, M. W. Beijersbergen, R. J. C. Spreeuw, and J. P. Woerdman, “Orbital angular-momentum of light and the transformation of Laguerre-Gaussian laser modes,” *Phys. Rev. A* **45**, 8185–8189 (1992).
18. A. T. O’Neil, I. MacVicar, L. Allen, and M. J. Padgett, “Intrinsic and extrinsic nature of the orbital angular momentum of a light beam,” *Phys. Rev. Lett.* **88**, 053601 (2002).
19. J. E. Curtis and D. G. Grier, “Structure of optical vortices,” *Phys. Rev. Lett.*, in press (2003).
20. M. J. Padgett and L. Allen, “The Poynting vector in Laguerre-Gaussian laser modes,” *Opt. Comm.* **121**, 36–40 (1995).
21. Standard results for Laguerre-Gaussian modes suggest that $R_\ell \propto \sqrt{\ell}$. These, however, do not account for diffraction by the objective lens’ aperture. See, for example, Refs. [10] and [17].
22. Hamamatsu, Corp. Model X7550 PAL-SLM.
23. S. C. Grover, A. G. Skirtach, R. C. Gauthier, and C. P. Grover, “Automated single-cell sorting system based on optical trapping,” *J. Biomed. Opt.* **6**, 14–22 (2001).
24. P. T. Korda, M. B. Taylor, and D. G. Grier, “Kinetically locked-in colloidal transport in an array of optical tweezers,” *Phys. Rev. Lett.* **89**, 128301 (2002).
25. M. E. J. Friese, T. A. Nieminen, N. R. Heckenberg, and H. Rubinsztein-Dunlop, “Optical alignment and spinning of laser-trapped microscopic particles,” *Nature* **394**, 348–350 (1998).